PCCP

Accepted Manuscript

ROYAL SOCIETY OF CHEMISTRY

www.rsc.org/pccp

Effective rate constant for nanostructured heterogeneous catalysts

Leila Rajabi[†] and S. C. Hendy[*,‡]

School of Chemical and Physical Sciences and MacDiarmid Institute for Advanced Materials and Nanotechnology, Victoria University of Wellington, PO Box 600, Wellington 6140, New Zealand, and Te Pūnaha Matatini, Department of Physics, University of Auckland, Private Bag 92019, Auckland 1142, New Zealand

E-mail: shaun.hendy@auckland.ac.nz

Abstract

There is a great deal of interest in the use of nanostructured heterogeneous catalysts, particularly those based on expensive precious metals, in order to maximise the surface to volume ratio of the catalyst, potentially reducing cost without sacrificing performance. When there is an abundance of reactant available, the effective reactivity will depend on the surface density of the catalytically active sites. However, under diffusion-limited conditions, catalytically active sites may compete for reactant, potentially leading to diminishing returns from the use of nanostructures. In this paper we apply a mathematical homogenization approach to investigate the effect of scale and patterning on the effective activity of catalytic sites on a heterogeneous catalyst operating under diffusion-limited condition. We test these theoretical results numerically

---

[*] To whom correspondence should be addressed

[†] School of Chemical and Physical Sciences and MacDiarmid Institute for Advanced Materials and Nanotechnology, Victoria University of Wellington, PO Box 600, Wellington 6140, New Zealand

[‡] Te Pūnaha Matatini, Department of Physics, University of Auckland, Private Bag 92019, Auckland 1142, New Zealand

using Monte Carlo simulations, and show that in the continuum limit the theory works well. In particular, in the limit where the mean free path is much less than the scale of patterning of catalytically active sites, the effective rate constant is found to be equal to the area-weighted harmonic mean of the rate constants on the surface. However, as the length scale of the patterns becomes comparable to the mean free path length, the simulations shows that the effective activity of the system can exceed the theoretical limit suggested by the continuum theory.

Introduction

Heterogeneous catalysis is of fundamental scientific interest in chemistry and materials science, as well as being of significant economic value to society.[1,2] The effective performance of a particular catalytic system can depend on the interplay between reactant availibility and the surface area the heterogeneous catalyst.[3] When there is a high concentration of reactants in the system, one would expect that the effective catalytic activity of a nanoparticulate catalyst by weight will increase with its surface area, suggesting that maximising the surface to volume ratio of such a catalyst could reduce its cost without sacrificing performance.[4–6] This has stimulated a great deal activity in the search to fabricate high-surface area nanoparticulate metal catalysts.[7]

However nanostructured catalysts do have their disadvantages. The high surface area of a nanostructured catalyst may reduce its stability, which can be a drawback when operating at high temperatures.[8] Furthermore, under diffusion-limited conditions, reactants may not be able to access the entire surface of a nanostructured catalyst[9,10] if the depletion zone of reactants about active sites on the catalyst start to overlap. Gas kinetic theory predicts that the size of this depletion zone will scale as the mean free path of the gas molecules,[11] so one might expect that under diffusion-limited conditions the effective reactivity of a heterogeneous catalyst would depend on the structure of the catalyst at that scale.

In this paper we consider the problem of computing the effective performance of a catalyst under diffusion-limited conditions, given a particular spatial arrangement of catalytically active sites on the catalyst surface. Indeed, the surface of a typical heterogenous catalyst will possess active sites with a range of activities distributed across a range of length scales. Under standard conditions, the mean free path of molecules in air is on the order of 100nm so we might expect that nanostructured catalysts may behave differently under diffusion-limited conditions to catalysts that are structured on larger or smaller length scales. In our model we consider a surface with a periodic array of active sites of period L. We describe the kinetics of the absorption of a reactant onto this catalytic surface using a Langmuir model, with the catalytic process described by a series of distinct elementary steps, including adsorption, reaction and desorption.

This theory developed here also applies to support that are covered by small catalytically-active particles.[12] Again, one may regard such a support as a catalyst with a heterogeneous distribution of active "sites", where in this case each "site" represents a catalytically active nanoparticle. In this case, one may have a great deal of control over how the particles are distributed over the support (e.g. see[13]) or indeed the distribution may change over time due to Ostwald ripening[14] or other process associated with the catalytic reaction.[15] Our approach allows one to compute the effective catalytic activity of a support in terms of its coverage by catalytically active particles.

We compute the effective activity of such surfaces under diffusion-limited conditions using two approaches. In the first, we use a continuum diffusion equation to describe the transport of reactants to the surface, and apply mathematical homogenization techniques[16,17] to compute an effective activity in a limit where the pattern period L is much less than the size of the depletion zone about the active sites, which is of order λ. The second approach is to use kinetic Monte Carlo simulations,[18] which allow us to test the predictions of the continuum approach, and observe the break down of the continuum approximation as the pattern period approaches the mean free path of the gas: $L \to \lambda$. We also investigate the effect of patterning of active sites on the catalyst surface (e.g. checkerboard and stripes).

The continuum theory predicts that for a given density of active sites, the performance of the catalyst depends only on the period of the pattern L and not the particular pattern. The kinetic Monte Carlo methods allow us to test this prediction in the limit where $L \sim \lambda$.

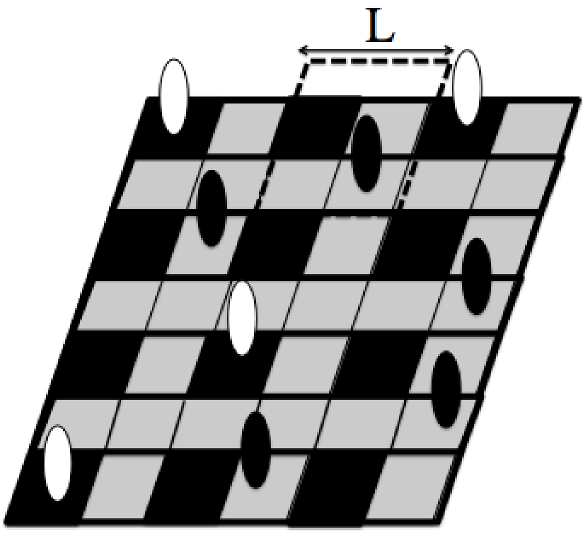

Figure 1: (An illustration of a catalyst surface, showing active sites (black) and non-active sites (grey) distributed in a pattern of period L with adsorbed particles (white) and non-absorbed particles (black).

Model and homogenization theory

We begin by describing the simple kinetic model used to describe the adsorption and catalytic processes that take place on the catalyst surface, as suggested by (Figure. 1). The catalyst surface consists of a patterned array of active sites, over which the activity can vary periodically with period L. We assume a Langmuir adsorption process, which is a simplest model of adsorption of materials onto a surface in which the only interactive forces are between the adsorbed molecules of the reactant and surface. We will also assume the system has reached steady-state and is operating under diffusion-limited conditions.

We also make a number of assumptions to simplify the mathematics. Once the reactants have adsorbed to the surface, we assume that they cannot diffuse on the surface before the catalytic reaction take place. In principle, desorption could occur, but in this work we will assume that the desorption rate is negligible. Likewise, we assume that the catalytic conversion process is also irreversible. These assumptions allow us to simplify the mathematical problem so that results from homogenization theory can be applied, although this comes at the expense of limiting the applicability of the model. For instance, we do not consider the possibility that the catalytically active sites are not the most favorable sites for adsorption.

We will consider a binary pattern on the surface, with low activity sites and high activity sites distributed periodically over the surface. Each site can only be occupied by one reactant molecule at a given time (Fig. 1).[3] We break the adsorption and catalytic processes down into four steps with associated rate constants k_1, k_2, k_3 and k_4 respectively:

1. Adsorption a gas particle of type A_g collides with an active site S_i and is adsorbed to this site with probability k_1:

$$A_g + S_i \to A_i,$$

2. The adsorbed particle desorbs from the surface to re-enter the gas phase without having undergone catalysis with rate k_2:

$$A_i \to A_g + S_i,$$

3. Adsorbed particles of type A are converted to particles of type B with rate k_3:

$$A_i \to B_i,$$

4. Particles of type B desorb from active sites with rate k_4:

$$B_i \to B_g + S_i,$$

To simplify the analysis, we will assume that step (4), the desorption of the reaction product B_{i}, occurs much more rapidly than the reaction step (i.e. $k_3 \ll k_4$) and that step (2), the desorption of the reactant is much slower than the reaction step (i.e. $k_2 \ll k_3$). With these assumptions, the step (3) is the rate limiting reaction step at the surface. Under these assumptions, the Langmuir equation for the fractional surface coverage θ_i of the site i is:

$$\frac{d\theta_i}{dt} = k_1 \left(1 - \theta_i\right) Q - k_3\theta_i, \tag{1}$$

where Q is collision rate per unit area over the entire surface. The first term is the rate of adsorption of particles that have diffused to the surface on an empty active site. The second term is the rate of catalytic conversion over the surface. Under diffusion-limited conditions, the fractional surface coverage $\theta_i \ll 1$, so the steady state will be given by:

$$\theta_i = \frac{k_1}{k_3} Q. \tag{2}$$

In order to proceed further, we need to introduce a model to describe the transport of the gas A to the catalyst surface. We use a Fickian diffusion equation, which describes the flux of gas A as it is consumed at the catalyst surface:

$$\frac{\partial \rho_A(r,t)}{\partial t} = D\nabla^2 \rho_A(r,t), \tag{3}$$

where D is the diffusion coefficient and ρ_A is the density of the gas A. Under steady-state conditions the density of gas A satisfies:

$$\nabla^2 \rho_A = 0. \tag{4}$$

Before a steady state is achieved, the coverage of the catalyst surface is a function of time and depends on the rate of adsorption and reaction of the reactants with the surface. Once a steady state is reached, the rate of adsorption becomes the same as the rate of conversion, and the particle influx at the catalyst surface Γ (with unit normal vector $\vec{n}$) is equal to the average density of converted particles per unit time:

$$-D\vec{n}\cdot\nabla\rho_A \mid_\Gamma = -\frac{d[B_g]}{dt} = \frac{k_3\theta_i}{a_i}, \tag{5}$$

where we have used the fact that $\frac{d[B_g]}{dt}$ is proportional to the second term on the right-hand side of (Eq. 1). By balancing the flux of gas A_g into the site i with the rate of adsorption of the gases by mass, we can obtain a steady-state boundary condition for the gas density, ρ_A over the surface:

$$-D\vec{n}\cdot\nabla\rho_A \mid_\Gamma = -\frac{k_1 Q}{1+\frac{k_1 Q a_i}{k_3}}, \tag{6}$$

where, according to gas kinetic theory, the collision rate is $Q = \frac{1}{4}\sqrt{\frac{8k_BT}{\pi m}}\rho_A \mid_\Gamma$, where m is the mass and T is the temperature of the gas A.

Under adsorption-limited conditions ($k_1 Q a_i \ll k_3$) the flux is proportional to the density of the gas A near the surface:

$$-D\vec{n}\cdot\nabla\rho_A \mid_\Gamma = -\frac{k_1}{4}\sqrt{\frac{8k_BT}{\pi m}}\rho_A, \tag{7}$$

which reduces to a simple mixed boundary condition for the density of gas A at the surface:

$$-l\vec{n}\cdot\nabla\rho_A \mid_\Gamma = \rho_A, \tag{8}$$

where the constant $l = \frac{D}{k_1}\sqrt{\frac{2\pi m}{k_BT}}$ has the dimension of length and can be interpreted as the size of the region over which the gas A is depleted by adsorption and catalysis at the surface. Gas kinetic theory tells us that $D \sim \lambda\bar{v}$ where $\bar{v} \sim \sqrt{\frac{k_BT}{m}}$ is the mean velocity of the gas molecules and λ is the mean free path of the gas molecules. As a consequence, the length l

is found to scale as the ration of mean free path to the probability of adsorption at an active site:

$$l \sim \frac{\lambda}{k_1}. \tag{9}$$

The discussion above, in particular the boundary condition (8), applies to a catalytic surface with a uniform distribution of active sites. However provided the distribution of active sites across the surface varies slowly enough, we would still expect (8) to hold, with $l \sim \lambda/k_1$ becoming a function of location on the surface. Conceptually we would regard the probability of absorption k_1 as varying across the surface on length scale $L \gg \lambda$. Regions with high k_1 would represent a high concentration of active sites on the surface, while regions with low k_1 would represent a low concentration of active sites.

We are interested in determining the *effective activity* of a catalytic surface with a density of active sites that varies over the surface. By effective activity, we mean the activity of a homogeneous surface (i.e. a surface with a constant k_1) that would produce the same overall rate of conversion of gas A as the heterogeneous surface when viewed macroscopically. To compute the effective activity, we use homogenization theory, which provides a proscription for obtaining the macroscopic properties of heterogeneous media in the presence of well-defined microstructure by averaging over microscopic scales.[19,20] In what follows, we assume that $l \sim \lambda/k_1$ varies periodically over the catalytic surface with period L.

In this case we expect $\rho_A/\nabla\rho_A \sim L$ near the surface. Consequently, it is convenient to introduce a dimensionless set of spatial coordinates $x^* = x/L$. The scaled boundary condition at the surface then becomes:

$$-\frac{l}{L}\vec{n} \cdot \nabla^* \rho_A(r,t) = \rho_A, \tag{10}$$

Thus the ratio of $L/l \sim (L/\lambda)\, k_1$ emerges as an important parameter in the effective performance of the catalyst.

By assuming (eq. 10) holds, two limiting cases can be examined. The first limit occurs when $l \ll L$, so that the boundary condition reduces to:

$$\rho_A = O(\frac{l}{L}). \tag{11}$$

which at zeroth order in l/L would give a purely diffusion-limited reaction. However by calculating the first order correction in l/L we can obtain an effective reactivity of the heterogeneous surface. By applying the asympototic homogenization method described in Ref.[20] (which amounts to making an expansion in powers of l/L and truncating at the first order), the effective activity of the catalyst surface (say, the plane defined by $z = 0$) is given by:

$$k_{eff} = \left\langle k_1(x, y)^{-1} \right\rangle^{-1} \tag{12}$$

to first order in l/L, where the angle brackets indicate the average of the quantity $k_1(x, y)$ over the surface. Note that in this case the effective activity is given by the area-weighted *harmonic* mean of k_1 rather than the arithmetic mean.

To examine the implications of (12), consider a surface composed of two types of region, with adsorption probabilities $k_a$and k_b respectively, that are periodically arranged over that surface. If a region of type a occupies an area fraction of ϕ on the surface, then the effective activity is given by:

$$k_{eff} = \frac{k_a k_b}{\phi k_b + (1 - \phi) k_a}. \tag{13}$$

If the coverages of the sites are such that $k_a/\phi \gg k_b/(1 - \phi)$ then this reduces to $k_{eff} \sim k_b/(1-\phi)$, so if the two regions occupy similar area fractions on the surface, but $k_a \gg k_b$, the effective absorption probability scales with the smaller value k_b. This is a direct consequence of the harmonic mean appearing in (12).

The second limit we consider occurs when $L \ll l$. Now the first-order boundary condition becomes

$$\vec{n}.\nabla\rho_A = O\Big(\frac{L}{l}\Big). \tag{14}$$

In this case it can be shown by homogenization (as shown in the Appendix) that the effective adsorption probability is given by:

$$k_{eff} = \big\langle k(x,y)\big\rangle. \tag{15}$$

where now instead of the harmonic mean we have the arithmetic mean of k_1.

Again it is instructive to consider a surface where reactants are more likely to adsorb in regions of type a than regions of type b (so $k_a > k_b$). If the coverage of the regions of type a is ϕ then $k_{eff} = \phi k_a + (1-\phi)k_b$. Again if are such that $k_a \gg (1-\phi)k_b/\phi$ then $k_{eff} \simeq \phi k_a$ so the effective absorption probability of the surface scales with the larger value k_a.

To summarise, homogenization theory predicts that the effective performance of a microstructured surface with adsorption probability Eqn. (7) will be that of a homogeneous surface with k_{eff}:

$$-D\sqrt{\frac{2\pi m}{k_B T}}\vec{n}\cdot\nabla\rho_A(r,t) = k_{eff}\rho_A, \tag{16}$$

where $k_{eff} = \Big\langle k_1(x,y)^{-1}\Big\rangle^{-1}$, the harmonic mean, when $L \gg l$ and $k_{eff} = \big\langle k(x,y)\big\rangle$, the arithmetic mean, when $L \ll l$. Note that in both cases the effective adsorption probability will be independent of the particular pattern of active sites on the catalyst surface. In the next sections we will test these predictions using kinetic Monte Carlo simulations. We will also examine their applicability away from the continuum limit. We note, however, that numerical solutions of the corresponding differential equations[21] verify that the effective activity calculated in the continuum limit is well-described by the expressions (12) and (15) in the appropriate limits. These numerical solutions also suggest that k_{eff} is bounded by the two limiting expressions at intermediate values of $L \sim l$.

Simulations

To test the theory developed in the previous section we have implemented the Langmuir adsorption model (processes (1-4)) together with lattice diffusion of the gas A near the surface using the kinetic Monte Carlo simulation method.[22] We consider a cubic $40 \times 40 \times 40$ lattice within a box with periodic boundary conditions in the x and y directions, and a catalytically active surface at the boundary $z = 0$.[23] The particles diffuse on the lattice, where the lattice constant is chosen to be equal to the mean free path λ of the gas A. At the top of the box we impose a reflecting boundary condition. The total number of particles in the simulation box is kept constant at 1600 by replacing particles that are converted with particles at the top of the simulation cell.

In the simulations presented here we have neglected process (2) (i.e. we have set $k_2 = 0$) and consider that process (4) is so rapid that it happens instantaneously (i.e. once conversion occurs we simply delete the particle from the catalyst surface). There is no interaction between the particles, except that only one active site on the surface can be occupied at any given time. This leaves three rates to consider in the simulations: $\tau_D^{-1} = D/\lambda^2$, the rate of diffusion in the gas; $k_1 Q$, the rate of adsorption; and $k_3 = \tau_c^{-1}$, the rate of conversion of adsorbed particles. The time constant (τ_D) is the mean free time of the diffusing gas particles, which we chose as our unit of time. The time constant (τ_c) is the relaxation time of the catalytic conversion process, which occurs only at occupied actives sites. These active sites on the catalyst surface ($z = 0$) are arranged in a periodic pattern or randomly distributed to achieve a specified surface coverage.

We use a rejection-free kinetic Monte Carlo method[24,25] to evolve the system to steady-state, which typically requires 10^6 Monte Carlo steps. This was checked to ensure that the particle flux at the catalyst surface had settled to some steady value and that the density gradient of the particles was approximately constant in the z-direction. We have considered spatial variations in $k_1(x, y)$ over the surface, while considering τ_c to be constant everywhere. We have tested patterns of different motif and coverage, together with variations in the period L. When $\tau_c \ll \tau_D$ the simulations can be used to test the expressions for the effective activity under diffusion-limited conditions given in the previous section (equations (12) and (15)).

Results

We first consider the continuum limit, $L \gg \lambda$, with $\tau_c \ll \tau_D$, where we would expect (12) to hold for finite values of k_1. In Figure 2 we consider the effective activity of a series of checker board patterns (such as those in the schematic in Fig. 1), where the period L is scaled from 2 to 20 λ and the surface coverage is varied from $\phi = 0$ to 1. All sites on the surface are active, but some have absorption probability $k_1 = 1.0$ (with surface coverage ϕ) while others have $k_1 = 0.5$ (with surface coverage $1 - \phi$). We choose $\tau_c = 0.1\tau_D$ constant over the entire surface. When $l \sim \lambda/k_1 \ll L$ we would expect equation (12) to hold. As shown in the figure, as L gets larger, the effective activity, and its dependence on the surface coverage, indeed approaches that predicted by equation (12). This illustrates the effectiveness of the homogenization approach in the continuum limit. Away from the continuum limit, when $L \sim l$ the theoretical expression underpredicts the effective reactivity. In fact, as $L \to \lambda$, k_{eff} is found to increase. In other words, for a fixed average coverage of active sites, surfaces with sites dispersed on scales comparable to λ are found to be more effective at capturing reactant than surfaces where sites are more concentrated.

It is also interesting to consider cases where $k_1 = 0$ on some parts of the surface, while k_1 is finite elsewhere. In figure 3 we again consider the effective activity for a series of checker board patterns as the period L increases from λ. Two curves are shown in the figure: in the first, $k_1 = 1.0$ on active sites, which have a coverage $\phi = 0.25$, while in the second, $k_1 = 0.8$

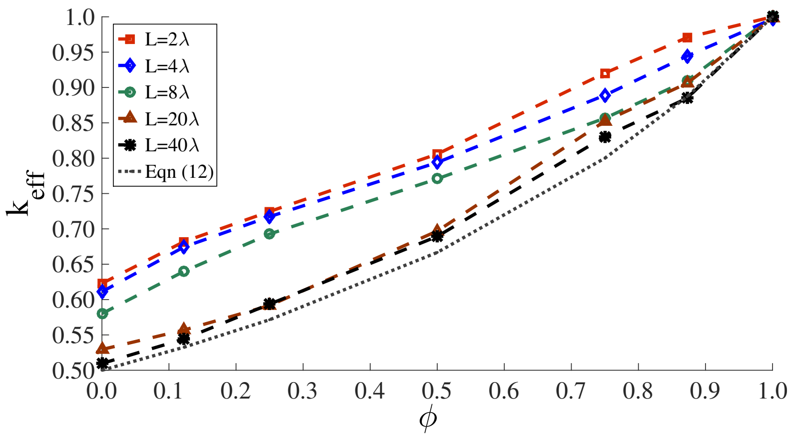

Figure 2: The figure compares the effective activities for a range of different domain sizes as a function of the surface coverage with effective reactivity predicted by equation (15). For length scales $L \sim \lambda$, the effective activity exceeds that predicted by (15) but as L gets larger, the effective activity is well described by equation (15).

on active sites, which have a coverage of $\phi = 0.5$. On all other sites $k_1 = 0$, so adsorption is not possible. Again $\tau_c = 0.1\tau_D$ over the entire surface, although now process (3) only occurs on active sites. In this case, we see that as $\lambda/L \to 0$ the effective activity k_{eff} approaches the value given by equation (15). Although $L \gg \lambda$ in this limit, over much of the surface $L \ll l \sim \lambda/k_1$ as $k_1 = 0$ and equation (15) seems to provide a good description of the effective activity. Away from the continuum limit, equation (15) again underestimates the effective activity of the surface.

Finally, we have considered the effect of different patterns, as well as the case where $\tau_c > \tau_D$, which is not covered by the theory developed in previous sections. We have considered a variety of patterns, as shown in the inset of figure 4, including a selection of checkerboard-type patterns, a pattern where active sites are randomly distributed over the surface, and stripes. As in the previous case, we find that for the larger domain sizes the effective activity is given by equation (15) for small τ_c, and that the effective activity of the patterns with smaller length scales exceed those predicted by the theory. As τ_C increases the effective activity decreases, as one might expect as the activity becomes reaction-limited rather than adsoprtion or diffusion-limited. Also note that the effective activity is pattern

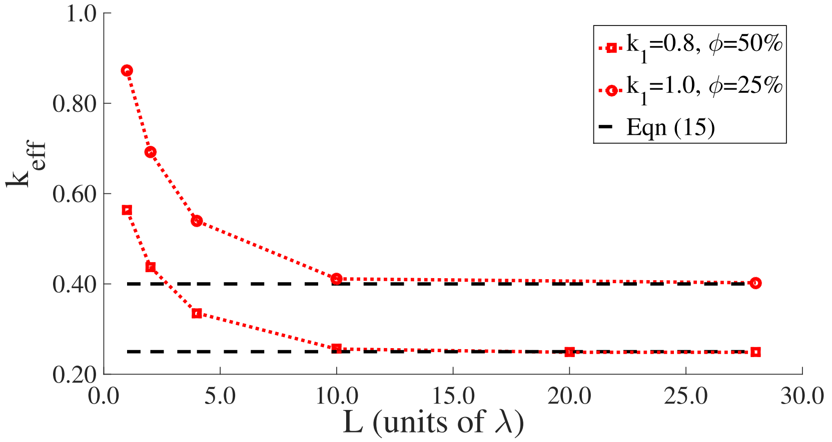

Figure 3: The relationship is shown between the effective activity k_{eff} and the domain size L is shown for the case where $k_1 = 0.8$ at 50% coverage (and $k_1 = 0$ elsewhere) and the case where $k_1 = 1.0$ at 25% coverage. The patterns here have a checkerboard character. The effective activity in the simulations approaches that predicted by equation (15) as $\lambda/L \to 0$ but exceeds this as $L \to \lambda$.

dependent, with the checked pattern with period $L = 2\lambda$ outperforming the stripes and the random pattern, which in turn outperform the patterns on larger length scales.

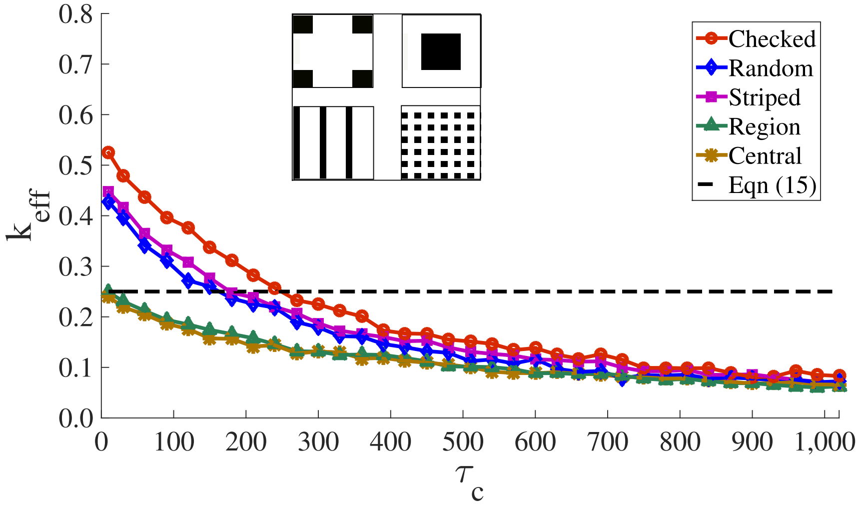

Figure 4: The figure shows the effective activity of different patterns with a surface coverage of active sites with $k_1 = 1.0$ of $\phi = 25\%$ and $k_1 = 0.0$ elsewhere as τ_C is varied. In the range of $0 < \tau_C \ll \tau_D$, the larger length length scale regions approach agreement with equation (15). For the patterns with periods comparable to the mean free path (λ), the effective activity exceeds the limit predicted by equation (15) as $\tau_C \to \tau_D$.

Discussion and conclusions

We have found that the two approximate expressions (12) and (15) for the effective catalytic activity of a surface with a heterogeneous distribution of catalytically active sites match the simulations well in the limits where they are expected to be valid. For distributions of active sites with length scales below the continuum limit we find that these expressions underestimate the effective activity. In air, under standard conditions, the mean free path of a gas molecule is of the order of 100 nm. Under these conditions, we would expect that the continuum diffusion equation (3) provides a good description of variations in the density of the gas at the catalyst surface on scales greater than 100 nm. Variations in the distribution of active sites below this scale would produce variations in the density of the reactant gas that would not be captured well by the continuum diffusion equations, as demonstrated by the kinetic Monte Carlo simulations presented here.

Nonetheless, the effects of variations in the distribution of active sites above this scale should be able to be captured by the continuum approach so it is interesting to consider the implications of the continuum theory. Consider a distribution of small but high activity particles (metal nanoparticles of diameter 10 nm, say, with $k_1 = k_a$) dispersed on larger, less active oxide particles (e.g 1μm TiO_2 particles, with $k_1 = k_b \ll k_a$) for instance.[26] Here we might find a variation of activity on length scales, L, of greater than 100 nm, so the continuum theory would be expected to be valid and equation (12) should hold. In this case the fractional enhancement to the effective activity of adding the small particles to the larger particles k_{eff}/k_b is proportional to $1/(1-\phi)$. The small particles essentially consume all the reactant they encounter, so it is their coverage rather than their activity that determines the enhancement to the effective activity of the larger particles.

In summary, we have applied a mathematical homogenization approach together with kinetic Monte Carlo simulations to investigate the effect of scale and patterning on the effective activity of catalytic sites on a heterogeneous catalyst operating under diffusion-limited conditions. The kinetic Monte Carlo simulations show that in the continuum limit the theory works well where applicable. In particular, in the limit where the mean free path is much less than the scale of patterning of catalytically active sites, the effective rate constant is found to be equal to the harmonic mean of the rate constant over the surface. However, as the length scale of the patterns becomes comparable to the mean free path length, the effective activity of the system can exceed the theoretical limit suggested by the continuum theory. We expect that this work will have implications for the design and use of nanostructured catalysts that need to operate under diffusion-limited conditions.

Acknowledgement

The authors would like to acknowledge the useful discussions that they had with Dr Nicola Gaston, Dr Philip Zhang and Dr Nathaniel Lund. They also acknowledge funding from the MacDiarmid Institute for Advanced Materials and Nanotechnology.

Appendix

In this appendix, we consider the homogenization of equation (10) in the limit where the period L becomes small compared to the far field. We introduce a function $\ell = \ell(x, y)$ which varies over the catalyst surface Γ_L. We assume that some appropriate boundary condition holds on some plane Γ_{far} in the far field, but will neglect it for the purposes of the calculation. The boundary condition of interest is:

$$-\ell(x, y)\vec{n} \cdot \nabla\rho = \rho, \quad \text{on the catalyst surface } \Gamma_L. \tag{17}$$

In weak form, with this boundary condition, equation (4) can be written:

$$2\int_{\Omega} \nabla\rho \cdot (\nabla u)\, dV + \int_{\Gamma_L} \frac{1}{\ell(x,y)} \rho\, u\, d\Gamma = 0 \tag{18}$$

where Ω is the domain bounded by the parallel planes Γ_L and Γ_{far} and u is an arbitrary test function. The homogenization limit is obtained when the the period $L/H \to 0$, where H is the far field distance (see[21] for instance). In this limit, one can consider a sequence of equations of the form of (18) each corresponding to a surface Γ_L with a smaller period L. In this limit the second term weakly converges to its average over a single period:

$$\int_{\Gamma_L} \frac{1}{\ell(x,y)} \rho\, u\, d\Gamma \to \int_{\Gamma_0} \left\langle \frac{1}{\ell(x,y)} \right\rangle \rho\, u\, d\Gamma \tag{19}$$

The strong form of this homogenized boundary condition, which will hold in the limit $L \ll l \ \sim H$, is thus

$$-\vec{n} \cdot \nabla\rho = \left\langle \frac{1}{\ell(x,y)} \right\rangle \rho, \quad \text{on}\, \Gamma_0. \tag{20}$$

Thus, in terms of k_1, we can write equation () in this limit as:

$$-D\sqrt{\frac{2\pi m}{k_B T}} \vec{n} \cdot \nabla\rho_A(r,t) = k_{eff}\rho_A, \tag{21}$$

where

$$k_{eff} = \langle k(x,y) \rangle. \tag{22}$$

References

(1) Zambelli, T.; Wintterlin, J.; Trost, J.; Ertl, G. *Science* **1996**, *273*, 1688–1690.

(2) Joo, S. H.; Park, J. Y.; Renzas, J. R.; Butcher, D. R.; Huang, W.; Somorjai, G. A. *Nano Lett* **2010**, *10*.

(3) Carberry, J. *Chemical and catalytic reaction engineering*; McGraw-Hill chemical engineering series; McGraw-Hill, 1976.

(4) Zhang, H.; Watanabe, T.; Okumura, M.; Haruta, M.; Toshima, N. *Nature Materials* **2012**, *11*, 49–52.

(5) Bell, A. T. *Science* **2003**, *299*, 1688–1691.

(6) Perez-Alonso, F. J.; McCarthy, D. N.; Nierhoff, A.; Hernandez-Fernandez, P.; Strebel, C.; Stephens, I. E. L.; Nielsen, J. H.; Chorkendorff, I. *Angewandte Chemie International Edition* **2012**, *51*, 4641–4643.

(7) Zhou, Z.-Y.; Tian, N.; Li, J.-T.; Broadwell, I.; Sun, S.-G. *Chem. Soc. Rev.* **2011**, *40*, 4167–4185.

(8) Hansen, T. W.; DeLaRiva, A. T.; Challa, S. R.; Datye, A. K. *Accounts of Chemical Research* **2013**, *46*, 1720–1730, PMID: 23634641.

(9) Flores-Camacho, J. M.; Fischer-Wolfarth, J. H.; Peter, M.; Campbell, C. T.; Schauermann, S.; Freund, H. J. *Phys Chem Chem Phys* **2011**, *13*, 16800–16810.

(10) Ilinitch, O. M.; Cuperus, F.; Nosova, L. V.; Gribov, E. N. *Catalysis Today* **2000**, *56*, 137 – 145.

(11) Chapman, S.; Cowling, T. G. *The mathematical theory of non-uniform gases: an account of the kinetic theory of viscosity, thermal conduction and diffusion in gases*; Cambridge university press, 1970.

(12) Astruc, D. *Nanoparticles and catalysis*; John Wiley & Sons, 2008.

(13) Lee, T.; Hendy, S. C.; Neto, C. *Nanoscale* **2015**, *7*, 2894–2899.

(14) Ouyang, R.; Liu, J.-X.; Li, W.-X. *Journal of the American Chemical Society* **2013**, *135*, 1760–1771, PMID: 23272702.

(15) Evans, J.; Tromp, M. *Journal of Physics: Condensed Matter* **2008**, *20*, 184020.

(16) Tritsaris, G. A.; Greeley, J.; Rossmeisl, J.; Norskov, J. K. *Catalysis Letters* **2011**, *141*, 909–913.

(17) Marc-Olivier Coppens, K. M. *Chemical Engineering Science* **2002**, *58*, 4787–4795.

(18) Voter, A. F. *Radiation Effects in Solids*; Springer, 2007; pp 1–23.

(19) Hendy, S. C.; Lund, N. J. *Phys. Rev. E* **2007**, *76*, 066313.

(20) Lund, N. J.; Zhang, X. P.; Mahelona, K.; Hendy, S. C. *Physical Review E* **2012**, *86*, 046303.

(21) Zhang, X.; Lund, N. J.; Hendy, S. C. *ANZIAM Journal* **2015**, *FirstView*, 10.

(22) Skakauskas, V.; Katauskis, P. *Journal of Mathematical Chemistry* **2012**, *50*, 141–154.

(23) Wolff, A.; Lohmar, I.; Krug, J.; Biham, O. *Physical Review E* **2011**, *10*.

(24) Schulze, T. P. *Journal of Computational Physics* **2008**, *227*, 2455–2462.

(25) Deutschmann., P. D. O. *First-Principles Kinetic Monte Carlo Simulations for Heterogeneous Catalysis: Concepts, Status, and Frontiers*; McGraw-Hill chemical engineering series; ed O. Deutschmann, 2011.

(26) Formo, E.; Lee, E.; Campbell, D.; Xia, Y. *Nano Letters* **2008**, *8*, 668–672, PMID: 18205427.